Activity and reusability of immobilized gold nanoparticles for the catalysis of both oxidation and reduction reactions

Célia Boukoufi, Ariane Boudier, Séphora Lahouari, Jean Vigneron, Igor Clarot

▶ **To cite this version:**

Célia Boukoufi, Ariane Boudier, Séphora Lahouari, Jean Vigneron, Igor Clarot. Activity and reusability of immobilized gold nanoparticles for the catalysis of both oxidation and reduction reactions. Results in Chemistry, 2023, 5, pp.100979. 10.1016/j.rechem.2023.100979 . hal-04119387

HAL Id: hal-04119387

https://hal.univ-lorraine.fr/hal-04119387

Submitted on 6 Jun 2023

HAL is a multi-disciplinary open access archive for the deposit and dissemination of scientific research documents, whether they are published or not. The documents may come from teaching and research institutions in France or abroad, or from public or private research centers.

L'archive ouverte pluridisciplinaire **HAL**, est destinée au dépôt et à la diffusion de documents scientifiques de niveau recherche, publiés ou non, émanant des établissements d'enseignement et de recherche français ou étrangers, des laboratoires publics ou privés.

Distributed under a Creative Commons Attribution - NonCommercial - NoDerivatives 4.0 International License

Results in Chemistry 5 (2023) 100979

Contents lists available at ScienceDirect

Results in Chemistry

journal homepage: www.sciencedirect.com/journal/results-in-chemistry

Activity and reusability of immobilized gold nanoparticles for the catalysis of both oxidation and reduction reactions

Célia Boukoufi [a,b], Ariane Boudier [a], Sephora Lahouari [a], Jean Vigneron [b], Igor Clarot [a,*]

[a] Université de Lorraine, CITHEFOR, F-54000 Nancy, France
[b] Pharmacy Department, University Hospital, 54511 Vandoeuvre-lès-Nancy, France

ARTICLE INFO

Keywords:
Gold nanoparticles
Nanostructured surface
Heterogeneous catalysis
P-nitrophenol
$DPPH^{\bullet}/DPPH_2$
Curcumin

ABSTRACT

Colloidal gold nanoparticles (AuNP) are well-known to present a catalytic activity. However, they are characterized by certain limitations, as a rather poor stability and lack of both handling and reusability. Their immobilization on surfaces could help to overcome these drawbacks. This work evaluated the impact of the immobilization of AuNP towards their catalytic activity on reduction and oxidation reactions. Colloidal AuNP stabilized with citrate ions were synthesized, characterized, and immobilized by the dip-coating method, the obtained immobilized AuNP (iAuNP) were characterized. The catalytic activity of AuNP and iAuNP was evaluated and compared to each other through the *p*-nitrophenol reduction reaction. The kinetic of the catalytic activity of iAuNP was slower than colloidal AuNP. The catalytic activity appeared to be impacted by the less available surface of iAuNP. The reduction efficiency of iAuNP was also evaluated with the $DPPH^{\bullet}/DPPH_2$ reduction reaction. The capacity of iAuNP to catalyze the reduction of $DPPH^{\bullet}$ in $DPPH_2$ was shown even after 130 days and 20 reuses of the nanostructured surface on the contrary to non-reusable colloidal AuNP. The oxidation efficiency of iAuNP was measured by the ability to catalyze the auto-oxidation of curcumin (HPLC-UV/vis). For all these experiments, the addition of 4-mercapto-phenol on the surface of iAuNP passivated the surface, decreasing the catalytic activity of the materials. In conclusion, iAuNP are redox catalysts with both anti- and pro-oxidant effects and high reusability over a very long period.

1. Introduction

For many years, gold has been considered to have no catalytic activity. This paradigm changed with the beginning of the nanoparticle era. The nanometric size increased the surface-to-volume ratio of gold and, consequently, drastically enhanced its reactivity. The first proof of the catalytic activity of gold nanoparticles (AuNP), was given in the 1980s, when, Masatake Haruta found that gold nanoparticles supported by metal oxides can catalyze the oxidation of carbon monoxide [1]. Nowadays, AuNP are easily synthesized and functionalized nanomaterials with controllable size and are wildly used [2]. They are described as "electron reservoir" redox catalysts [3] and still intensively studied for their catalytic activity [4]. At the colloidal state, their catalytic properties are put to good use in many fields such as biology [5], chemistry [6] and environment [7].

However, at the colloidal state, AuNP have certain limitations. For example, they have a limited stability depending on the pH, the ionic strength of the medium leading to their aggregation and thus to the loss of their properties [8]. Moreover, when added to the reaction medium, AuNP cannot be easily recovered from the medium and are, therefore, used only once [9]. These drawbacks could be overcome using immobilized AuNP (iAuNP) on surfaces, creating nanostructured materials for heterogeneous catalysis. The immobilization could help to increase the stability of AuNP in several media [10] while taking profit of their unique properties and easily removing them from the reaction medium. The reusability and handling of such materials could be an important advantage over colloidal AuNP.

Several methods can be used to immobilize NP on surfaces. The dip-coating is one of the simplest, cheapest and most reproducible method, in which the substrate/surface is immersed in successive baths with

Abbreviations: 4MP, *p*-mercaptophenol; AuNP, Gold nanoparticles; BHT, Butylated hydroxytoluene; $DPPH^{\bullet}$, 1,1-diphenyl-2-picrylhydrazyl; $DPPH_2$, 1,1-diphenyl-2-picrylhydrazine; HPLC-UV/vis, High-Performance Liquid Chromatography with Ultra-Violet and visible detection; iAuNP, Immobilized gold nanoparticles; *p*-AP, *p*-aminophenol; *p*- NP, *p*-nitrophenol; PEI, Polyethylenimine; FIB-SEM, Focused Ion Beam Scanning Electron Microscope; SPR, Surface Plasmon Resonance.

* Corresponding author.
E-mail address: igor.clarot@univ-lorraine.fr (I. Clarot).

https://doi.org/10.1016/j.rechem.2023.100979
Received 5 April 2023; Accepted 26 May 2023
Available online 30 May 2023
2211-7156/© 2023 The Authors. Published by Elsevier B.V. This is an open access article under the CC BY-NC-ND license (http://creativecommons.org/licenses/by-nc-nd/4.0/).

different coating components. In the case of AuNP immobilization, the substrate is soaked first in a polymer solution and then in a colloidal suspension of AuNP. Due to their negatively charged surface, AuNP can create electrostatic interactions with oppositely charged polymers [11]. The avidity of gold for sulfur atom is also used for the immobilization of AuNP on surface. These two solutions can also be combined, by using 2-iminothiolane (Traut's reagent) that allows to attach thiol groups on polymers bearing primary amines [12].

But do AuNP retain their properties after immobilization? The immobilization modifies the environment of AuNP [13] and lowers the availability of their surface, that can affect their catalytic activity [14]. The purpose of this study is to evaluate the catalytic activity of AuNP before and after their immobilization on glass slides. The catalytic activity of AuNP and iAuNP was measured using the *p*-nitrophenol/ *p*-aminophenol (*p*-NP/*p*-AP) reduction reaction and compared. AuNP are also known to be able to catalyze both reduction and oxidation [15], we investigated whether the immobilization of the AuNP could sustain these activities. The reduction efficiency of iAuNP has been evaluated through the reduction of 1,1-diphenyl-2-picrylhydrazyl picrylhydrazyl in 1,1-diphenyl-2-picrylhydrazine ($DPPH^{\bullet}/DPPH_2$) [16]. Then, curcumin which is a well-known "antioxidant" molecule [17] is highly sensitive to oxidation. Its autoxidation is initiated by hydrogen abstraction and leads to the formation of bicyclopentadione as the final product [18]. The oxidation of curcumin was used to measure oxidation efficiency of iAuNP compared to AuNP and a common antioxidant (butylated hydroxytoluene, BHT).

As a control and to evaluate the significance of the availability of the AuNP surface of iAuNP, *p*-mercaptophenol (4MP) was capped at the surface of nanostructured glass slides. It is made of a phenolic hydroxyl and a thiol group [19]. The thiol group allows its binding to AuNP through gold-thiol bound [20]. The activity of AuNP with 4MP was evaluated simultaneously with the other iAuNP to evaluate whether the addition of a molecule at the surface of iAuNP impact their activity.

For each tested reaction, the catalytic activity of iAuNP was demonstrated and the kinetics was slowed down. Very interestingly, a long-term reusability of iAuNP was proved determined, with a catalytic activity existing of up to 130 days of continuous testing.

2. Material and method

2.1. Reagents and standards

All reagents and solvents were of analytic grade and used without further purification. Ultrapure deionized water (greater than18.2 MΩ cm) was used for the preparation of all solutions. Methanol, *p*-nitrophenol, 2-iminothiolane hydrochloride and ammonia solution 25 % were purchased from Carlo Erba, Fluka, Alfa Aesar and Riedel de Haen, respectively. Branched poly-(ethylene imine) (PEI) (average molecular masses of 80,000) was purchased from Sigma Aldrich as all other reagents.

2.2. Synthesis of citrate-capped gold nanoparticles

Citrate-capped AuNP were synthesized according to our previous work [21]. Briefly, under an inert atmosphere (N_2) and stirring (250 rpm), 1 mL of $AuCl_4^-$ aqueous solution (25 mM) was added to 90 mL of ultrapure water, giving a final concentration of 270 μM of gold. Two milliliters of sodium citrate (55 mM) were added and then, after exactly 1 min, 1 mL of $NaBH_4$ (19.5 mM). The solution was stirred for another 5 min. The resulting suspension was stored in the dark at + 4 °C for a maximum of 20 days [21].

2.3. Gold nanoparticle characterization

The absorbance (A_{AuNP}) and spectra recordings of colloidal AuNP were measured by UV–Visible spectrophotometer (UV-2600 Shimadzu). The concentration of AuNP (C_{AuNP} (mol.L^{-1}), was calculated according to Lambert–Beer's law Eq. (1):

$$A_{AuNP} = \varepsilon_{AuNP} l \times C_{AuNP} \quad (1)$$

AuNP have a molar absorbance value of $\varepsilon_{AuNP} = 1.2 \times 10^7\ M^{-1}.cm^{-1}$ (taken at the maximum wavelength which is the Surface Plasmon Resonance (SPR) band), determined by our laboratory [22]. The final concentration of synthesized AuNP was 59± 3 nM expressed in AuNP. The number of AuNP (n_{AuNP}) was calculated using Avogadro's number (N_A (mol^{-1})), according to Eq. (2):

$$n_{AuNP} = C_{AuNP} \times N_A \quad (2)$$

The hydrodynamic diameter in volume mode (D_h) and zeta potential (ζ) of AuNP were measured at 25 ± 1 °C with a Zetasizer Nano ZS (Malvern Instruments, UK). Transmission Electron Microscopy (TEM) images were recorded using a Philips CM20 instrument with a LaB_6 cathode at 200 kV.

2.4. Immobilization of gold nanoparticles

Scheme 1 illustrates the process of immobilization of AuNP on a glass slide, with a theoretical and schematic representation of the modification of the glass slide surface after each step. First, 24 × 36 mm borosilicate glass slides (Menzel-Gläser) were cleaned and activated at 100 °C with, first, a 15-min bath in an aqueous solution of 0.1 M sodium dodecyl sulfate and, then with another 15-min bath 0.1 M HCl solution. They were then rinsed with ultrapure water and dried [23].

Branched polyethyleneimine (PEI), a cationic polymer, and 2-iminothiolane solutions were prepared at 0.1 and 0.01 M, respectively, in 10.0 mL of 0.15 M, Tris − HCl buffer pH = 7.4. Tris − HCl buffer was obtained by dissolving 18.2 g of Trizma® base in 1 L of H_2O, pH was adjusted to pH = 7.4. The coatings were made by soaking slides 10 min, first, in the PEI solution and then in a bath of 2-iminothiolane solution. These two steps allowed the immobilization of AuNP through electrostatic interactions and gold-sulfur bond, respectively. Finally, they were immersed in a last bath of colloidal AuNP. The last bath was repeated 1, 5, 15, or 30 times (corresponding to 1, 5, 15, or 30-iAuNP respectively) (Scheme 1). After each bath, glass slides were rinsed with Tris − HCl buffer (3 min) and water. The AuNP colloidal suspensions were used for 5 deposits and then renewed [23].

Some 15-iAuNP were dipped in a 0.13 M solution of 4MP dissolved in 0.15 M Tris − HCl buffer pH = 8.1 for 10 min and rinsed (corresponding to 4MP-15iAuNP).

2.5. Characterization of immobilized gold nanoparticles

The nanostructured glass slides were characterized using UV–vis spectrophotometer for absorbance measurements and spectra recordings. For Ion Beam Scanning Electron Microscope (FIB-SEM) (Helios Nanolab 600i and FEI brand), the surface of the nanostructured glass slide was directly observed without metallization. The ion-emitting gallium source was set to 20 kV on the nanostructured glass slides. For TEM (Philips CM20 instrument with a LaB_6 cathode at 200 kV), carbon covered copper grids (Agar) were nanostructured following the previously described dip coating protocol, but decreasing the incubation time from 10 and 3 min to 3 and 1 min, respectively.

Quantification of AuNP immobilized on glass slides was performed according to a method, adapted and validated by our laboratory [21]. Briefly, nanostructured glass slides were crushed, put in contact with an HCl-NaCl-Br_2 solution (1.0 M – 0.3 M – 0.025 M respectively) and stirred to oxidize the AuNP. The suspending solution was partially evaporated (Turbovap, Biotage). Then, NH_4Cl (30 % m/V), HCl (6 M), and Rhodamine B (0.084 μM) solutions were added to allow the formation of ion pairs between tetrachloroaurate anions and the Rhodamine B. The ion-pairs were extracted with diisopropyl ether. This organic phase was completely evaporated. The dried residue was dissolved in HPLC mobile

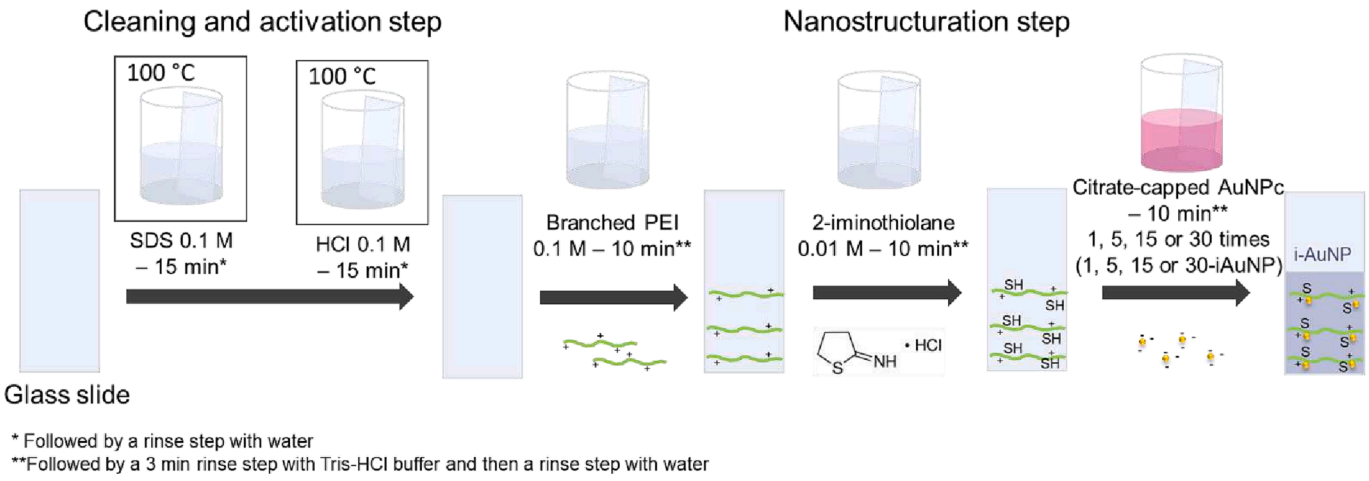

Scheme 1. Immobilization of gold nanoparticles.

phase (acetonitrile and 0.1% trifluoroacetic acid aqueous solution (25/75, V/V)) before injection. HPLC was performed on a Shimadzu LC-20 system (degasser (SCM1000), quaternary pump (LC 20AD), autosampler (SIL 20AC)). The UV–vis detector (SPD20A) was set at 555 nm. The column (Macherey Nagel Nucleosil 100–3 C18, 150/4.6) was heated at 40 °C (Croco-cil oven). The injection volume was 100 µL and the flow rate was 1.0 mL.min^{-1}. Data acquisition was performed using Shimadzu LabSolution.

2.6. Catalysis of the reduction of p-NP by immobilized gold nanoparticles

The catalytic activity of AuNP and iAuNP was evaluated using the *p*-NP/*p*-AP reduction reaction [24]. For the colloidal nanoparticles, 15 µL of colloidal AuNP at final concentrations of 9, 19, 45, 68 and 90 × 10^{-12} M were added in 5 mL of aqueous solution of *p*-NP (0.1 mM) and 5 mL of aqueous solution of $NaBH_4$ (0.1 M). For iAuNP, the nanostructured glass slides were directly dipped in the solution of *p*-NP and $NaBH_4$. Control was made of p-NP with $NaBH_4$ without iAuNP. The experiment was conducted at 20 ± 2 °C, under stirring (*ca.* 150 rpm). The catalytic performance was followed by using a UV − Vis spectrophotometer. The concentration of the reactant (*p*-NP) and the product (*p*-AP) were followed at 400 and 300 nm, respectively, and measured at t = 0, 5, 10, 20, 30, 40, 50, and 60 min.

A pseudo-first-order rate law was considered (Eq (3)) for the calculation of the constant of kinetic, k, which was calculated as the value of the slope of Eq (4):

$$C = C_0.\exp^{-kt} \quad (3)$$

$$Ln\,C = -kt\,.\ln C_0 \quad (4)$$

in which C is the concentration of *p*-NP at a time t calculated using Beer Lambert's law with ε = 9.19× 10^3 L.mol^{-1}.cm^{-1}, C_0 is the initial concentration.

The reduction efficiency (E_R) was calculated by the following Eq (5):

$$E_R = (C0 - C1)/C0 \times 100 \quad (5)$$

where C0 is the concentration of *p*-NP in the control, and C1 is the concentration of *p*-NP in the sample, after 1 h.

2.7. Catalysis of the reduction of 1,1-diphenyl-2-picrylhydrazyl by immobilized gold nanoparticles and reusability

The stock solution of DPPH$^•$ was prepared in methanol (710 µM). The working solution (71 µM) was obtained by dilution in methanol-10 mM / citrate ammonium buffer pH 7.4 (60/40, V/V), a solvent mixture that does not alter the iAuNP. Ammonium citrate buffer was obtained by dissolving 2.1 g of citric acid in 1 L of H_2O, pH was adjusted to pH = 7.4 with ammonia solution 25 %. Nanostructured glass slides were immersed in 10 mL of working solution. The samples were placed in the dark at 37 °C and under a stirring of *ca.* 50 rpm. The reduction of DPPH$^•$ into $DPPH_2$ was studied by following the absorbance at 515 nm ($\varepsilon_{DPPH•}$ = 11.08× 10^3 L.mol^{-1}.cm^{-1}) at t = 0, 1, 2, 3, 4, 5, and 6 h.

In parallel, positive controls were realized with reduced glutathione as a reference antioxidant (*ca.* 5 mg), and the negative control was realized with only DPPH$^•$ solution incubated in similar conditions (without iAuNP). The activity of glass slides covered with PEI-Traut coating (without AuNP) was also evaluated.

The reduction efficiency (E_R) was calculated by the following Eq (6):

$$E_R = (A0 - A1)/A0 \times 100 \quad (6)$$

where A0 is the absorbance of the negative control, and A1 is the absorbance of the sample, after 6 h.

The reusability of iAuNP was evaluated on the 30 iAuNP. For this purpose, 30iAuNP was used a total of 20 times to reduce DPPH$^•$ into $DPPH_2$, over a period of 130 days.

2.8. Catalysis of the oxidation of curcumin by immobilized gold nanoparticles

The stock solution of curcumin was prepared in methanol (1.0 mM) was diluted 20 times with a methanol-10 mM citrate ammonium buffer pH 7.4 (60/40, V/V). Ten milliliters of curcumin solution (50 µM) were stored alone and in presence of 39 µM solution of antioxidant (butylated hydroxytoluene (BHT)) (controls), or in contact with 5, 15, 30, 4MP-15iAuNP or both 5iAuNP and 39 µM BHT. The samples were stored at 20 ± 2 °C, at room light, and stirred at *ca.* 150 rpm. The concentrations of curcumin were measured at t = 0, 7, 14, and 21 days using an HPLC-UV/vis (Shimadzu LC-10) method.

The Shimadzu LC-10 system was constituted by a quaternary pump (LC-10AT), an autosampler (SIL-10AD), and an UV–DAD detector (Spectra System UV600 LP). The column (Macherey Nagel Nucleosil 100–5 C18, 250/4.5) was at 40 °C (Croco-cil oven). Data acquisition was performed by the ChromQuest software. The isocratic mobile phase was composed of acetonitrile and ultrapure water (45/55, V/V) with 0.1 % of formic acid. The injection volume was 10 µL. The detector was set at wavelengths of 280 nm (for degradation products) and 425 nm (for curcumin) [25]. The pump was set at a flow rate of 1.0 mL.min^{-1}.

A first-order rate law, described in Eq (3), was considered for the calculation of the kinetic constant.

The half-life was calculated using Eq (7) and the oxidation efficiency

(E_O) according to Eq (8):

$$t_{1/2} = \ln(2)/k \quad (7)$$

In which $t_{1/2}$ is the half-life of curcumin and k being the kinetic constant.

$$E_O = (C0 - C1)/C0 \times 100 \quad (8)$$

where C0 is the concentration of curcumin in the negative control, and C1 is concentration of curcumin in the sample, after 21 days.

3. Results and discussion

3.1. Characterization of colloidal gold nanoparticles

The citrate-capped AuNP had a concentration of 59 ± 5 nM and showed a surface plasmon resonance (SPR) at λmax = 512 ± 2 nm (Fig. 1(a)). Their hydrodynamic and core diameters were 6.2 ± 0.9 nm (Fig. 1(b)) and 2.7 ± 0.9 nm (Fig. 1(d)), respectively. The citrate ions at the surface of AuNP led to a negative surface charge of – 30 ± 6 mV (Fig. 1(c)). This characterization was in concordance with our previously published results [21,22]. (Fig. 1 (d)).

3.2. Characterization of immobilized gold nanoparticles

AuNP were immobilized on the surface of glass slides using the dipping method. Branched PEI is polycationic positively charged at pH = 7.4 (in aqueous solution, pKa = 3.3, 6.7, 9.2, and 9.9 at 25) polymer [26] that adsorbs to glass slide by electrostatic interactions with the help of silanol groups [11]. The bath in 2-iminothiolane allowed the formation of thiol groups and a positive charge from the primary amino groups of PEI [27]. Both the positive charges and the presence of sulfur atoms enabled the immobilization of the negatively charged citrate-capped AuNP via electrostatic interactions and gold-sulfur bonds [28], respectively.

The resulting iAuNP had a SPR visible through spectroscopic measurements (Fig. 2(a) and (b)), that confirmed the presence of AuNP at the nanoparticle state. The value of the SPR increased with the number of deposits and reached a plateau after the 10th deposit (Fig. 2 (b)). In parallel, the absorbance of iAuNP was also intensified with the number of deposits due to the increasing of the total number of immobilized AuNP from 1 to 30 deposits (Fig. 2(c)). The modification of the SPR reflected the increasing number of neighbors of each AuNP and, in parallel, the decreasing distance between each AuNP [29]. However, in comparison with colloidal AuNP, no modification of the size of AuNP has been observed in TEM, and each AuNP was still well individualized (Fig. 2(d) compared to Fig. 1(d)). The material was homogenously covered by the AuNP as demonstrated by MEB (Fig. 2(e)). For 30-iAuNP, $14.6 \pm 4.4 \times 10^{13}$ AuNP were deposited at the surface of the glass slide, which corresponded to a density of 1.69×10^{13} AuNP/cm^2 (Table 1).

Alongside, some 15-iAuNP were covered with 4MP. After the immersion of 15-iAuNP in the solution of 4MP, its SPR shifted from 580.6 ± 0.5 nm to 624.6 ± 2.3 nm (Fig. 2(f)). The SPR of AuNP is influenced by their size, their shape and also their environment and/or surface chemistry [26]. Therefore, the modification of the SPR confirmed the effective adsorption of 4MP on the surface of the 4MP-15iAuNP.

3.3. Catalysis of the reduction of p-NP by immobilized gold nanoparticles

The catalytic activity of AuNP and iAuNP was tested by their impact on the reduction of *p*-NP. The addition of $NaBH_4$ in a solution of *p*-NP led to the formation of the nitrophenolate ion that showed maximum absorbance at 400 nm. In the presence of a catalyst, the nitrophenolate ion was then reduced in *p*-AP, that had an absorption band at 300 nm (Fig. 3(a)) In the absence of a catalyst, the reduction of p-nitrophenolate ions by $NaBH_4$ proceeds very slowly, Ning *et al.* showed that there was no significant reduction before 10 h of reaction under these conditions [27]. In this work, the initial concentration of p-nitrophenolate ions was measured stable without any loss over the first hours of reaction, thus allowing to highlight the proper activity of either AuNP or iAuNP.

In this section and for a sake of clarity, the results were expressed in term of "total number of AuNP" to allow the comparison between

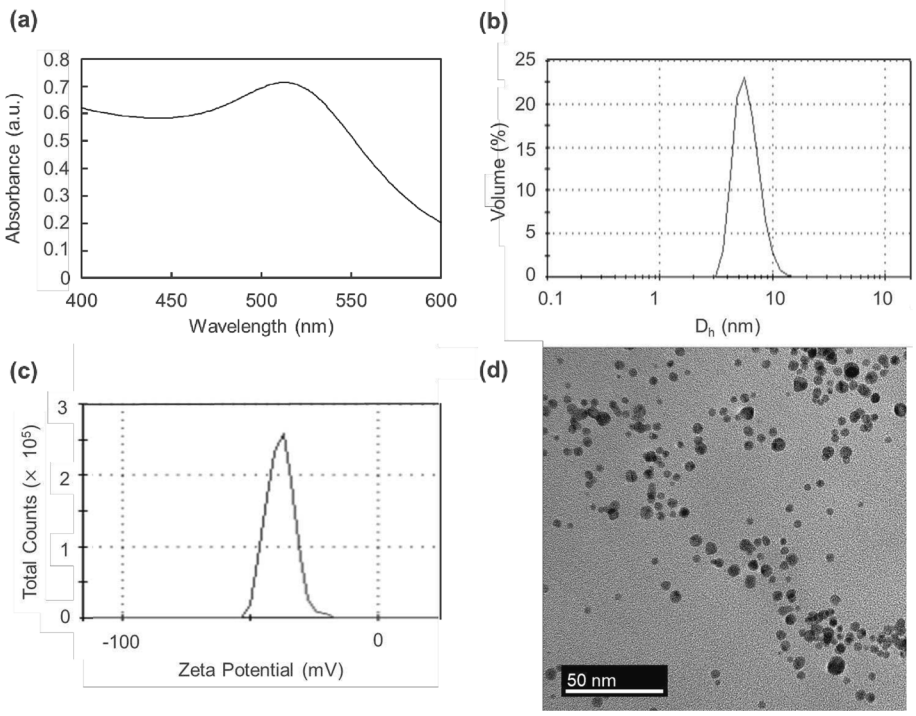

Fig. 1. Physicochemical characterization of colloidal AuNP using (a) spectrophotometry, (b) Dynamic Light Scattering (DLS), (c) DLS coupled to Laser Doppler Electrophoresis, (d) TEM picture of colloidal AuNP.

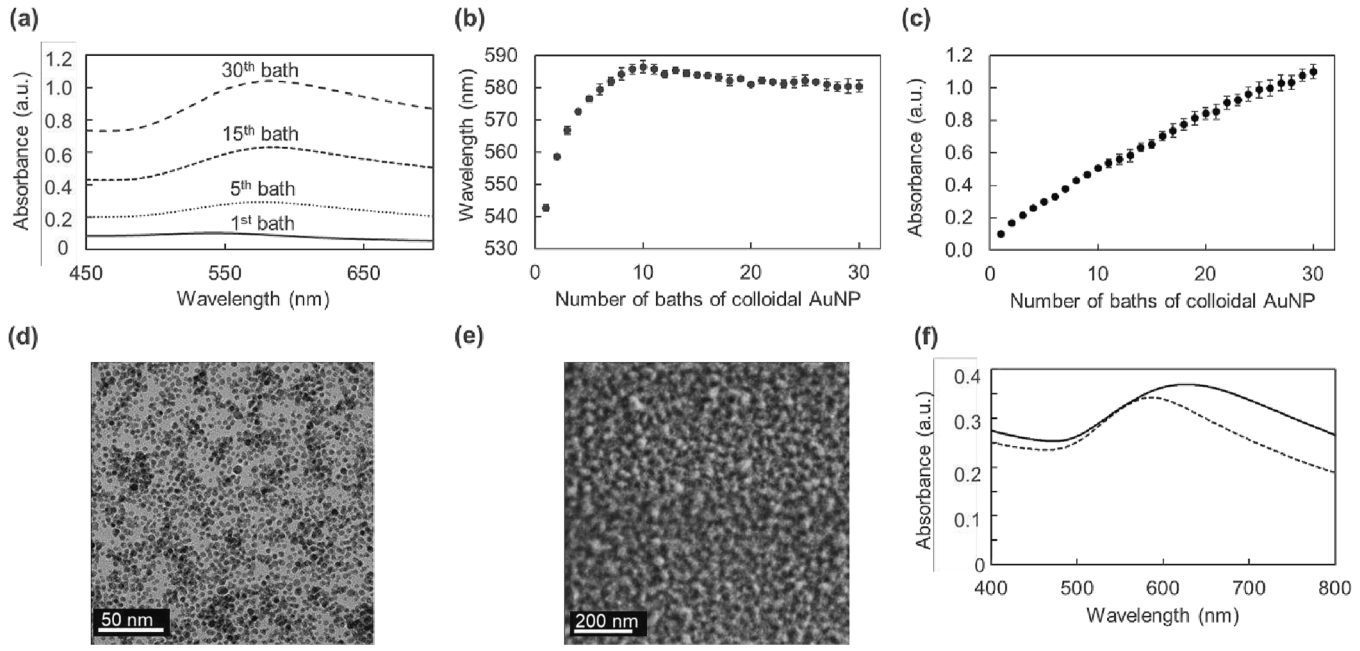

Fig. 2. Characterization of iAuNP: (a) Spectra recorded during iAuNP preparation; (b) SPR according to the number of baths of colloidal AuNP; (c) Absorbance at the SPR according to the number of bath of AuNP; (d) TEM picture of 15-iAuNP; (e) MEB picture of 30-iAuNP; (f) Spectra of 15iAuNP (dotted line) and 4MP-15iAuNP (continuous line).

Table 1
Catalytic constant of the p-nitrophenol reaction (k) and reduction efficiency (ER) of iAuNP and AuNP after 1 h at 20 °C.

iAuNP / AuNP	Number of AuNP ($\times 10^{13}$)	k (min^{-1}) ($\times 10^{-2}$)	ER (%)
1-iAuNP	1.2 ± 0.1	2.9 ± 0.1	83.3 ± 1.3
5-iAuNP	3.2 ± 0.1	2.5 ± 0.3	80.7 ± 2.8
15-iAuNP	5.4 ± 0.4	2.6 ± 0.2	80.3 ± 2.2
30-iAuNP	14.6 ± 4.4	2.2 ± 0.2	74.2 ± 2.3
4MP-15iAuNP	5.4 ± 0.4	0.4 ± 0.2	25.3 ± 10.4
Colloidal AuNP	0.005	0.2 ± 0.2	87.2 ± 1.7
	0.010	0.4 ± 0.1	70.8 ± 3.0
	0.026	0.8 ± 0.2	41.1 ± 5.1
	0.040	2.0 ± 1.5	25.3 ± 4.2
	0.053	10.0 ± 0.2	15.7 ± 7.7

colloidal and iAuNP.

The addition of AuNP in the mixture of *p*-NP and $NaBH_4$ led to the gradual decrease in the absorbance at 400 nm, and thus in the concentration of *p*-NP. In parallel, a gradual increase in the absorption band at 300 nm was observed, which corresponded to the formation of *p*-AP (Fig. 3(a)). This decrease was dependent of the number of added AuNP (Fig. 3(b)). Without the addition of AuNP, the absorbance at 400 nm of the *p*-NP remains stable for 60 min (Control in Fig. 3(b)). These results brought in light the catalytic activity of colloidal AuNP. Moreover, the kinetic constant of the catalytic reaction (k) of colloidal AuNP increased exponentially with the amount of AuNP (Fig. 3(c)).

The purpose of this work was to evaluate the impact of the immobilization towards the catalytic activity of AuNP. This activity was similar whatever the number of deposits (Fig. 3(d) and Table 1). The yields obtained in this study (more than 80 %) were in accordance with other published works [28,29]. No activity was observed for the glass slide without AuNP (control in Fig. 3(d), $k = 0.05 \pm 0.07 \times 10^{-2}\ min^{-1}$).

The activity of 5, 15 and 30-iAuNP, that contained at their surface more than 10^{13} AuNP, was comparable with the activity of a 100-fold smaller amount of colloidal AuNP (4.0×10^{11}) (Table 1).

The immobilization seemed to slow down the catalytic activity of AuNP. The immobilization of AuNP limited their Brownian motion in comparison to their colloidal state. Their reactivity may also be limited by the electronical interaction between the polymer and the electronic cloud at the surface of AuNP [23]. A model of the catalytic reduction of *p*-NP on the surface of AuNP, already suggested that the reaction depended on the total surface area of the AuNP available [30].

The importance of the availability of the AuNP surface was also demonstrated since the capping of i-AuNP by MP lowered by a factor of 6.5 the reactivity of 4MP-15iAuNP (Fig. 3d and Table 1). *P*-mercaptophenol at the surface of iAuNP has OH groups that formed H-bound to each other [20]. This reduces the accessibility of the electronic cloud on the surface of the gold atoms and consequently reduces their activity. Chen *et al.* have also demonstrated the modulation of the catalytic activity according to the availability of the AuNP. They developed poly(N-isopropylacrylamide)-coated gold nanoflowers whose activity depended on the temperature. The temperature modulated the conformation of poly(N-isopropylacrylamide) and thus the availability of the gold nanoflowers surface. When the polymer was uncoiled, the availability was reduced and consequently was the catalytic activity [31].

p-NP is also one of the most common organic-pollutants in industrial wastewater [32]. The reduction of *p*-NP in *p*-AP (an intermediate in the synthesis of dyes or pharmaceuticals) offers at the same time the degradation of a toxic compound and the formation of a high-value product [33]. The catalytic activity of iAuNP besides the other advantages (stability and handling), seems compatible with an application as *in situ* reactor. They could be usable for the degradation of chemical compounds, making them a potential tool for wastewater treatment.

3.4. Catalysis of the reduction of 1,1-diphenyl-2-picrylhydrazyl by immobilized gold nanoparticles and reusability

The DPPH•/ $DPPH_2$ method is commonly used to evaluate the radical scavenging activity of substances according to Eq (9):

$$DPPH^{\cdot} + Reduced\ molecule \rightleftharpoons DPPH_2 + Oxidized\ molecule \quad (9)$$

In the literature, this test is often employed to demonstrate the antioxidant activity of colloidal AuNP [34–36] but the catalytic contribution of AuNP in this reaction is not always broached in these studies [37]. The radical scavenging activity of colloidal citrate-capped AuNP is already known: their half maximal effective concentration (EC_{50}) has

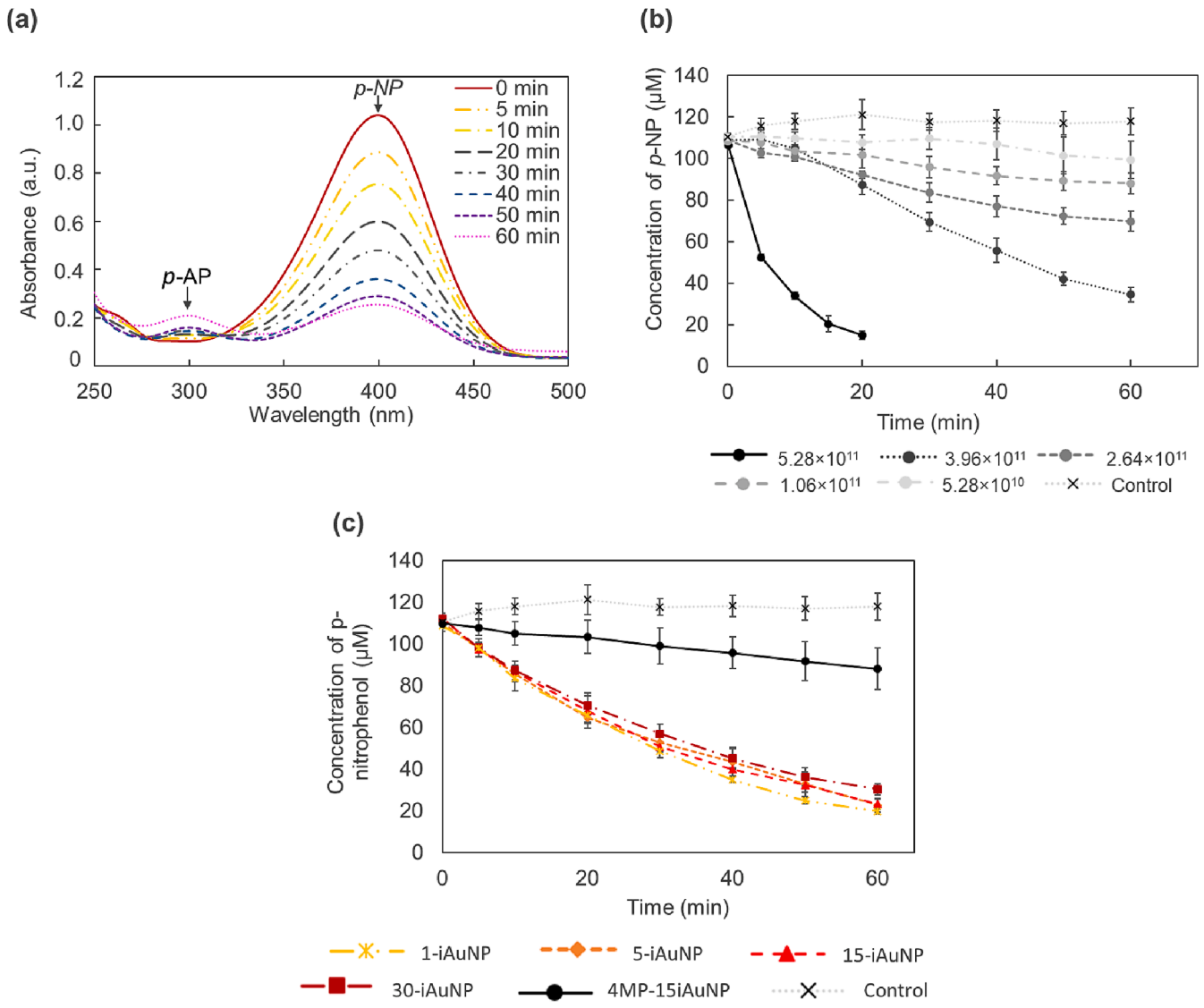

Fig. 3. (a) UV–vis spectra of the reduction of p-NP to p-AP at different times in presence of 15-i AuNP at 20 °C; (b) Evolution of the concentration of the p-NP concentration in presence of an increasing total number of colloidal AuNP at 20 °C; (c) Evolution of the concentration of the p-NP concentration in presence of iAuNP at 20 °C (n = 3). The control is made of 10 mL of reagent solution without AuNP.

been measured at 11 ± 1 nM [38]. The radical scavenging activity can also be viewed through the prism of catalysis and be considered as the catalysis of a reduction reaction, which has been done in this work.

All the tested iAuNP (from 5 to 30 deposits) catalyzed the reduction of $DPPH^{\bullet}$ in $DPPH_2$ with the reduction efficiency mentioned in Table 2. This activity is only due to AuNP, since glass slide without AuNP did not have any effect (E_R = -1.3 ± 2.0 %). Again, the reduction efficiency of 4MP-15iAuNP was *ca* 2.5 times lower than 15-iAuNP even if they present the same amount of AuNP. The passivation process induced by 4MP in 4MP-15iAuNP was in accordance with its reduced catalytic activity as the one described for the reaction with p-NP.

Unlike the catalytic activity on *p*-NP, the reduction efficiency increased with the number of deposits and thus with the total number of AuNP with a concentration-dependent effect. Catalytic activity is usually not concentration-dependent, unless the minimum quantity necessary for the effect is not provided.

Reuse of iAuNP was studied on 30iAuNP over a 130-day period for 20 reductions of $DPPH^{\bullet}$ (Table 4). The reduction efficiency of 30iAuNP slowly decreased during the first 6 days (corresponding to 6 reuses), and then reached a plateau in which the reduction efficiency remained significant (41.8 ± 5.8 %) until 130 days (or 20 uses). This result highlighted the improvement provided by the immobilization of AuNP.

This result highlights the improvement brought by AuNP immobilization, which allows the removal and preservation of the nanostructured catalytic surface, and surface and makes it suitable for many reuses. In comparison, colloidal AuNP could be used only once as they are not recoverable. They are dramatically less stable than iAuNP (21 vs 130 days). In addition, the reduction efficiency of colloidal AuNP could not be evaluated using the DPPH• method, because the reaction takes place in a mix of aqueous buffer and methanol in which AuNP in their colloidal state aggregate. All these considerations highlight once again the greater stability and the major interest of iAuNP compared to colloidal AuNP, for a catalytic use independent of their environment

Table 2
Reduction efficiency (ER) of iAuNP (n = 3) after 6 h.

Glass slide	E_R(%)
5-iAuNP	22.0 ± 0.6
15-iAuNP	37.2 ± 3.6
4MP-15-iAuNP	15.4 ± 4.2
30-iAuNP	76.2 ± 0.6

(medium, solvent).

3.5. Impact of immobilized gold nanoparticles on the stability of curcumin

The ability of iAuNP to catalyze oxidation was studied by following the concentration of curcumin using HPLC-UV/vis. The three main peaks observed at 425 nm at (Fig. 4(a)) corresponded to curcumin (tr = 18.6 ± 0.0 min) and two main impurities, bisdemethoxycurcumin and desmethoxycurcumin at 15.1 ± 0.4 and 16.8 ± 0.0 min, respectively [40]. As a function of time, the concentration of these three molecules decreased, and peaks corresponding to degradation products appeared which were mainly visible at 280 nm (Fig. 4(b)).

The main factor affecting the stability of curcumin is auto-oxidation [18]. Both 5,15 and 30-iAuNP showed a catalytic activity inducing the oxidation of curcumin, as described in Fig. 4(c) and Table 3. The addition of iAuNP induced a 2.5-fold faster degradation of curcumin (Table 4). Curcumin did not seem to adsorb on iAuNP. If that had happened, we would have had a decrease in the activity of iAuNP. An absence of catalytic activity was observed for 4MP-15iAuNP proving the passivation of the nanostructured surface by MP. To confirm that iAuNP effectively catalyzed the auto-oxidation of curcumin, BHT, a chain-breaking or radical-trapping antioxidant, was added. It slows down (or blocks) the auto-oxidation by competing with the propagation reaction [41]. At 39 μM, BHT did not impact the stability of curcumin. However, it significantly protected curcumin from 5 to iAuNP induced degradation and decreased the its oxidation efficiency by 40% (Fig. 4(d) and Table 4), confirming that iAuNP actually catalyzed curcumin auto-oxidation.

The stability of the nanostructured slides was evaluated by direct quantification of the gold present on their surface during the oxidation study of curcumin. Over the 21 days of study, no significant loss of gold was observed, indicating again a very good stability of the iAuNP. This result is in accordance with the one obtained in Section 3.4.

Table 3
Reduction efficiency (ER) of 30-iAuNP (n = 3) during 130 days.

Day	E_R(%)
0	76.2 ± 0.6
1	72.1 ± 1.1
2	62.2 ± 6.2
3	52.6 ± 4.8
5	47.5 ± 4.1
130	41.8 ± 5.8

Table 4
Half-life of curcumin at 21 days stored exposed to light at 20 °C alone (control) or in contact with 5, 15 or 30-iAuNP, 4MP-15iAuNP, 39 μM BHT or both 39 μM BHT and 5-iAuNP, kinetic constant (k) and oxidation efficiency (EO) (n = 3).

Glass slide	Half-life (days)	k ($days^{-1}$) ($\times 10^{-2}$)	E_O (%)
Control	17.2 ± 1.0	4.1 ± 0.2	
BHT 39 μM	18.7 ± 1.1	3.7 ± 0.2	
5-iAuNP + 39 μM BHT	10.4 ± 0.3	6.7 ± 0.2	47.0 ± 2.3
5-iAuNP	6.2 ± 0.2	11.2 ± 0.3	77.5 ± 1.9
15-iAuNP	6.1 ± 0.2	11.4 ± 0.3	84.0 ± 2.1
30-iAuNP	8.5 ± 1.8	8.4 ± 1.9	57.3 ± 14.2
4MP-15-iAuNP	17.3 ± 1.0	3.8 ± 0.1	6.2 ± 2.0

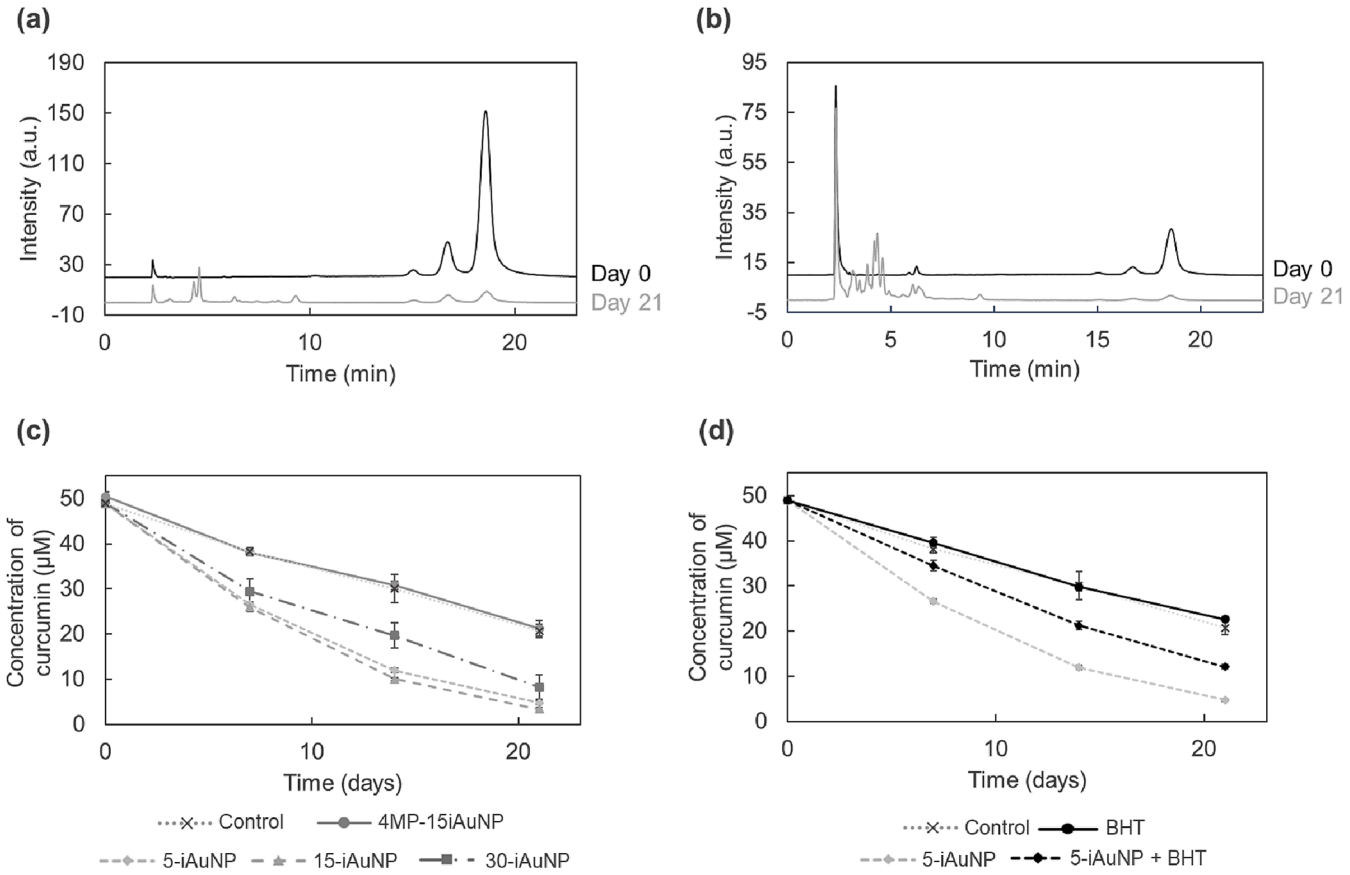

Fig. 4. Chromatograms of curcumin at day 0 (grey) and 21 (black) when stored in contact with 5 iAuNP with a detection at 425 nm (a) and 280 nm (b); (c) Concentration of curcumin at 21 days stored exposed to light at 20 °C alone (control) or in contact with 5, 15 or 30-iAuNP or 4MP-15iAuNP, please notice that the curves of the control and 4MP-iAuNP are overlaid; (d) Concentration of curcumin at 21 days stored exposed to light at 20 °C alone (control) or in contact with 39 μM BHT, 5-iAuNP or both, please notice that the curves of the control and BHT 39 μM are overlaid (n = 3).

4. Conclusion

In this work AuNP were successfully immobilized at the surface of glass slides. We demonstrated that iAuNP could catalyze both oxidation and reduction reactions. The obtained gold nanostructured surface showed a catalytic activity evaluated using the *p*-NP reduction reaction. Indeed, on the one hand, iAuNP catalyzed the reduction of $DPPH^{\bullet}$ in $DPPH_2$, and on the other hand, its catalytic activity promoted the auto-oxidation of curcumin. Even if the immobilization decreased the catalytic activity of iAuNP in comparison with colloidal AuNP from a kinetic point of view, it allowed iAuNP to present a greater stability and an important reusability with an activity kept after 130 days and 20 reuses. The obtained long-lasting multi-catalytic iAuNP is a promising tool in a multitude of fields such as biology or health. Due to the apparent non-specificity of the catalyzed reaction, they could be used as *in situ* reactor for various heterogenous catalysis, such as for the treatment of waste water [39], the formation of active pharmaceutical ingredient from a pro-drug [40] or biosensing [41].

CRediT authorship contribution statement

Célia Boukoufi: Conceptualization, Data curation, Investigation, Methodology, Writing – original draft, Writing – review & editing. **Ariane Boudier:** Conceptualization, Methodology, Supervision, Writing – original draft, Writing – review & editing. **Sephora Lahouari:** Investigation, Writing – review & editing. **Jean Vigneron:** Writing – review & editing. **Igor Clarot:** Conceptualization, Methodology, Supervision, Writing – original draft, Writing – review & editing.

Declaration of Competing Interest

The authors declare that they have no known competing financial interests or personal relationships that could have appeared to influence the work reported in this paper.

Data availability

No data was used for the research described in the article.

References

[1] M. Haruta, T. Kobayashi, H. Sano, N. Yamada, Novel Gold Catalysts for the Oxidation of Carbon Monoxide at a Temperature far Below 0 °C, Chem. Lett. 16 (1987) 405–408, https://doi.org/10.1246/cl.1987.405.

[2] S. Siddique, J.C.L. Chow, Gold Nanoparticles for Drug Delivery and Cancer Therapy, Appl. Sci.-Basel. 10 (2020) 3824, https://doi.org/10.3390/app10113824.

[3] R. Ciganda, N. Li, C. Deraedt, S. Gatard, P. Zhao, L. Salmon, R. Hernández, J. Ruiz, D. Astruc, Gold nanoparticles as electron reservoir redox catalysts for 4-nitrophenol reduction: a strong stereoelectronic ligand influence, Chem. Commun. 50 (2014) 10126–10129, https://doi.org/10.1039/C4CC04454A.

[4] M. Abbas, H.H. Susapto, C.A.E. Hauser, Synthesis and Organization of Gold-Peptide Nanoparticles for Catalytic Activities, ACS Omega 7 (2022) 2082–2090, https://doi.org/10.1021/acsomega.1c05546.

[5] J.G. Heddle, Gold Nanoparticle-Biological Molecule Interactions and Catalysis, Catalysts 3 (2013) 683–708, https://doi.org/10.3390/catal3030683.

[6] T. Mitsudome, K. Kaneda, Gold nanoparticle catalysts for selective hydrogenations, Green Chem. 15 (2013) 2636–2654, https://doi.org/10.1039/c3gc41360h.

[7] A. Quintanilla, S. Garcia-Rodriguez, C.M. Dominguez, S. Blasco, J.A. Casas, J. J. Rodriguez, Supported gold nanoparticle catalysts for wet peroxide oxidation, Appl. Catal. B-Environ. 111 (2012) 81–89, https://doi.org/10.1016/j.apcatb.2011.09.020.

[8] A. Albanese, W.C.W. Chan, Effect of Gold Nanoparticle Aggregation on Cell Uptake and Toxicity, ACS Nano 5 (2011) 5478–5489, https://doi.org/10.1021/nn2007496.

[9] L. Tang, X. Wang, B. Guo, M. Ma, B. Chen, S. Zhan, S. Yao, Salt-triggered liquid phase separation and facile nanoprecipitation of aqueous colloidal gold dispersion in miscible biofluids for direct chromatographic measurement, RSC Adv. 3 (2013) 15875–15886, https://doi.org/10.1039/C3RA40676H.

[10] A. Pallotta, M. Parent, I. Clarot, M. Luo, V. Borr, P. Dan, V. Decot, P. Menu, R. Safar, O. Joubert, P. Leroy, A. Boudier, Blood Compatibility of Multilayered Polyelectrolyte Films Containing Immobilized Gold Nanoparticles, Part. Part. Syst. Char. 34 (2017) 1600184, https://doi.org/10.1002/ppsc.201600184.

[11] A. Pallotta, I. Clarot, J. Beurton, B. Creusot, T. Chaigneau, A. Tu, P. Lavalle, A. Boudier, Analytical strategy for studying the formation and stability of multilayered films containing gold nanoparticles, Anal. Bioanal. Chem. 413 (2021) 1473–1483, https://doi.org/10.1007/s00216-020-03113-6.

[12] R. Singh, L. Kats, W.A. Blättler, J.M. Lambert, Formation of N-substituted 2-iminothiolanes when amino groups in proteins and peptides are modified by 2-iminothiolane, Anal. Biochem. 236 (1996) 114–125, https://doi.org/10.1006/abio.1996.0139.

[13] P.A. Atmianlu, R. Badpa, V. Aghabalaei, M. Baghdadi, A review on the various beds used for immobilization of nanoparticles: Overcoming the barrier to nanoparticle applications in water and wastewater treatment, J. Environ. Chem. Eng. 9 (2021) 106514. https://doi.org/10.1016/j.jece.2021.106514.

[14] M. Biswas, E. Dinda, M.H. Rashid, T.K. Mandal, Correlation between catalytic activity and surface ligands of monolayer protected gold nanoparticles, J. Colloid Interface Sci. 368 (2012) 77–85, https://doi.org/10.1016/j.jcis.2011.10.078.

[15] J. Lou-Franco, B. Das, C. Elliott, C. Cao, Gold Nanozymes: From Concept to Biomedical Applications, Nano-Micro Lett. 13 (2020) 10, https://doi.org/10.1007/s40820-020-00532-z.

[16] M.C. Foti, Use and Abuse of the DPPH(•) Radical., Journal of Agricultural and Food, Chemistry 63 (40) (2015) 8765–8776.

[17] T. Ak, I. Gulcin, Antioxidant and radical scavenging properties of curcumin, Chem.-Biol. Interact. 174 (2008) 27–37, https://doi.org/10.1016/j.cbi.2008.05.003.

[18] O.N. Gordon, C. Schneider, Vanillin and ferulic acid: not the major degradation products of curcumin, Trends Mol. Med. 18 (2012) 361–363, https://doi.org/10.1016/j.molmed.2012.04.011.

[19] J. Chen, J. Yang, L. Ma, J. Li, N. Shahzad, C.K. Kim, Structure-antioxidant activity relationship of methoxy, phenolic hydroxyl, and carboxylic acid groups of phenolic acids, Sci. Rep. 10 (2020) 2611, https://doi.org/10.1038/s41598-020-59451-z.

[20] H. Bian, J. Li, H. Chen, K. Yuan, X. Wen, Y. Li, Z. Sun, J. Zheng, Molecular Conformations and Dynamics on Surfaces of Gold Nanoparticles Probed with Multiple-Mode Multiple-Dimensional Infrared Spectroscopy, J. Phys. Chem. C 116 (14) (2012) 7913–7924.

[21] A. Pallotta, A. Boudier, B. Creusot, E. Brun, C. Sicard-Roselli, R. Bazzi, S. Roux, I. Clarot, Quality control of gold nanoparticles as pharmaceutical ingredients, Int. J. Pharm. 569 (2019), 118583, https://doi.org/10.1016/j.ijpharm.2019.118583.

[22] J. Tournebize, A. Sapin-Minet, R. Schneider, A. Boudier, P. Maincent, P. Leroy, Simple spectrophotocolorimetric method for quantitative determination of gold in nanoparticles, Talanta 83 (5) (2011) 1780–1783.

[23] J. Beurton, I. Clarot, J. Stein, B. Creusot, C. Marcic, E. Marchioni, A. Boudier, Long-lasting and controlled antioxidant property of immobilized gold nanoparticles for intelligent packaging, Colloids Surf. B Biointerfaces 176 (2019) 439–448, https://doi.org/10.1016/j.colsurfb.2019.01.030.

[24] M.T. Alula, H. Spende, T.A. Aragaw, A.N. Alene, B.A. Aragaw, M. Madiba, A Highly Stable Silver Nanoparticle Loaded Magnetic Nanocomposite as a Recyclable Catalysts, J. Clust. Sci. (2022), https://doi.org/10.1007/s10876-022-02386-4.

[25] T. Esatbeyoglu, K. Ulbrich, C. Rehberg, S. Rohn, G. Rimbach, Thermal stability, antioxidant, and anti-inflammatory activity of curcumin and its degradation product 4-vinyl guaiacol, Food Funct. 6 (2015) 887–893, https://doi.org/10.1039/C4FO00790E.

[26] P.K. Jain, X. Huang, I.H. El-Sayed, M.A. El-Sayad, Review of some interesting surface plasmon resonance-enhanced properties of noble metal nanoparticles and their applications to biosystems, Plasmonics 2 (2007) 107–118, https://doi.org/10.1007/s11468-007-9031-1.

[27] Y. Ning, Y. Guan, W. Song, F. Zhang, L. Chen, F. Chai, Preparation of Cu-W Nanoflakes and their Catalytic Performance for the Hydrogenation of 4-Nitrophenol, ChemistrySelect 8 (2023) e202203194.

[28] J.-H. Kim, K.M. Twaddle, J. Hu, H. Byun, Sunlight-Induced Synthesis of Various Gold Nanoparticles and Their Heterogeneous Catalytic Properties on a Paper-Based Substrate, ACS Appl. Mater. Interfaces 6 (2014) 11514–11522, https://doi.org/10.1021/am503745w.

[29] Y. Wang, P. Gao, Y. Wei, Y. Jin, S. Sun, Z. Wang, Y. Jiang, Silver nanoparticles decorated magnetic polymer composites (Fe3O4@PS@Ag) as highly efficient reusable catalyst for the degradation of 4-nitrophenol and organic dyes, J. Environ. Manage. 278 (2021), 111473, https://doi.org/10.1016/j.jenvman.2020.111473.

[30] M. Li, G. Chen, Revisiting catalytic model reaction p-nitrophenol/NaBH4 using metallic nanoparticles coated on polymeric spheres, Nanoscale 5 (2013) 11919–11927, https://doi.org/10.1039/C3NR03521B.

[31] C. Chen, D.Y.W. Ng, T. Weil, Polymer-grafted gold nanoflowers with temperature-controlled catalytic features by in situ particle growth and polymerization, Mater. Chem. Front. 3 (2019) 1449–1453, https://doi.org/10.1039/C9QM00252A.

[32] Toxicological Profile for Nitrophenols: 2-nitrophenol, 4-nitrophenol, U.S. Department of Health & Human Services, Public Health Service, Agency for Toxic Substances and Diseases Registry, 1992.

[33] S. Fu, G. Ren, S. Li, F. Chai, C. Wang, F. Qu, Morphology tuning of assembled Au–Cu nicotinate rings by ligand coordination and their use as efficient catalysts, New J. Chem. 41 (2017) 1509–1517, https://doi.org/10.1039/C6NJ03790A.

[34] Z. Nie, K.J. Liu, C.-J. Zhong, L.-F. Wang, Y. Yang, Q. Tian, Y. Liu, Enhanced radical scavenging activity by antioxidant-functionalized gold nanoparticles: A novel inspiration for development of new artificial antioxidants, Free Radic. Biol. Med. 43 (2007) 1243–1254, https://doi.org/10.1016/j.freeradbiomed.2007.06.011.

[35] S. Priya Velammal, T.A. Devi, T.P. Amaladhas, Antioxidant, antimicrobial and cytotoxic activities of silver and gold nanoparticles synthesized using Plumbago zeylanica bark, J. Nanostruct. Chem. 6 (2016) 247–260, https://doi.org/10.1007/s40097-016-0198-x.

[36] N. Muniyappan, M. Pandeeswaran, A. Amalraj, Green synthesis of gold nanoparticles using Curcuma pseudomontana isolated curcumin: Its

characterization, antimicrobial, antioxidant and anti- inflammatory activities, Environ. Chem. Ecotoxicol. 3 (2021) 117–124, https://doi.org/10.1016/j.enceco.2021.01.002.

[37] M.H. Oueslati, L.B. Tahar, A.H. Harrath, Catalytic, antioxidant and anticancer activities of gold nanoparticles synthesized by kaempferol glucoside from Lotus leguminosae, Arab. J. Chem. 13 (2020) 3112–3122, https://doi.org/10.1016/j.arabjc.2018.09.003.

[38] J. Tournebize, A. Boudier, A. Sapin-Minet, P. Maincent, P. Leroy, R. Schneider, Role of Gold Nanoparticles Capping Density on Stability and Surface Reactivity to Design Drug Delivery Platforms, ACS Appl. Mater. Interfaces 4 (2012) 5790–5799, https://doi.org/10.1021/am3012752.

[39] M. Sagir, M.B. Tahir, Role of Nanocatalyst (Photocatalysts) for Waste Water Treatment, Curr. Anal. Chem. 17 (2021) 138–149, https://doi.org/10.2174/1573411016666200226091404.

[40] Z. Chen, H. Li, Y. Bian, Z. Wang, G. Chen, X. Zhang, Y. Miao, D. Wen, J. Wang, G. Wan, Y. Zeng, P. Abdou, J. Fang, S. Li, C.-J. Sun, Z. Gu, Bioorthogonal catalytic patch, Nat. Nanotechnol. 16 (2021) 933–941, https://doi.org/10.1038/s41565-021-00910-7.

[41] W. Xu, L. Jiao, Y. Wu, L. Hu, W. Gu, C. Zhu, Metal-Organic Frameworks Enhance Biomimetic Cascade Catalysis for Biosensing, Adv. Mater. 33 (2021) 2005172, https://doi.org/10.1002/adma.202005172.